Anti-parallel sliding in Active Ising Model

Yash Rana
Applied Physics, Harvard John A. Paulson School Of Engineering And Applied Sciences

Emergent behaviour of Active Matter arises from interacting self-propelled constituents driven out of equilibrium by energy consumption. Active nematics, self-propelled agents with nematic alignment, are ubiquitous in nature and are an interesting realization of Active Matter [1]. In this project, I modify the Active Ising Model (AIM) developed by Solon et al [2] in an attempt to capture the phenomenology of Active Nematics. Using their random sequence update algorithm ([3]) I simulate the modified AIM to show the existence of states of meta-stable bands of opposite polarization. I derive a mean-field theory and discuss the affect of introducing fluctuations by numerically estimating the associated phase diagram. Finally, I discuss the apparent miss-match between the phase diagrams estimated from my simulations and the refined mean field theory.

I. INTRODUCTION

Modelling the collective behaviour of active matter reveals minimal components required to give rise to the phenomena and gives interesting physical insights into the universality of collective behaviour in nature. The earliest theoretical treatments of active matter modelled the interacting components with microscopic rules inspired by biological flocking (Reynolds [4] and Viseck [5]), see figure (1). A popular set of microscopic rules is that each self-propelled moving at constant speed chooses its direction based on the direction of motion of its neighbour up to some noise ([5]).

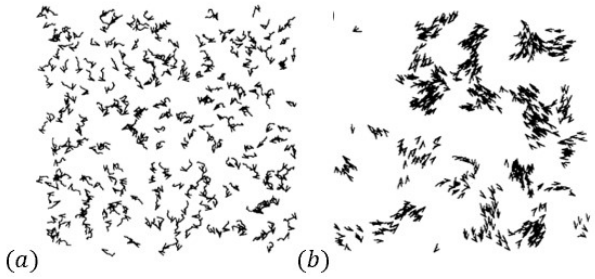

FIG. 1. Simulations of self-propelled boids moving at constant speed where each particle follows the average direction of it's neighbours gives rise to collective flocking. (a) has more orientational noise than (b). Borrowed from Fig 1 of ([5])

Coarse graining of the microscopic interactions led to the development of hydrodynamic theories of active matter ([6], [7]). An alternate strategy to the hydrodynamic approach are Active Lattice Models ([2],[8]), where active polar constituents sit on lattice sites. Such a treatment quantitatively captures all the features of the original Viseck Model. However, it is unclear if such Active Ising models can describe active nematics.

Active nematics present are a unique subset o self-propelled particles where particles align with others soley based on their nematic order. Real examples of 2D Active Nematics, e.g. microtubule-motor-protein mixtures, are well studied experimentally [9] and display aesthetically appealing turbulent flows, where pairs of +1/2 and -1/2 defect emerge, propel and annihilate each other, see figure (2).

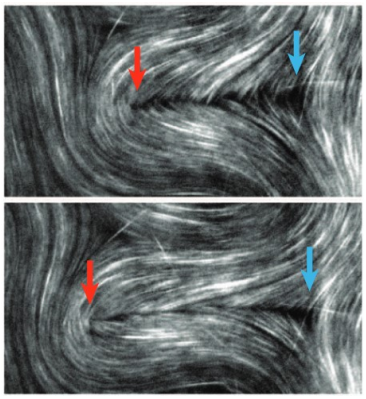

FIG. 2. Exotic dynamics of 2D streaming active nematics confined to fluid interfaces. The figure also shows the active dynamics of topological defect +1/2 (red arrow) propelling away from -1/2 defect (blue arrow). Borrowed from Fig 3 of ([9])

In this project, I modified the microscopic rules of an Active Ising model [3] to describe Active Nematics. Note, however, that the Simha-Ramaswamy instability [10] that leads unstable flows in ([9]) arise due to coupling with hydrodynamic flows hence a-priori one can not expect a dry active matter model as discussed here to reproduce the above phenomena.

II. MODEL

A. Motivation for microscopic rules

To model the phenomenology of active nematics, at least in spirit, we look at the active molecular processes that occur on microtubules, and polar rods which build the cytoskeletal structures like the mitotic spindle, see figure (3). We pick two key processes: (a) Kinesin-5 driven anti-parallel sliding and (b) dynein-driven -ve end clustering which would cause microtubules to align. To simplify our system, we assume that the length of microtubules is fixed (i.e. they are stabilized).

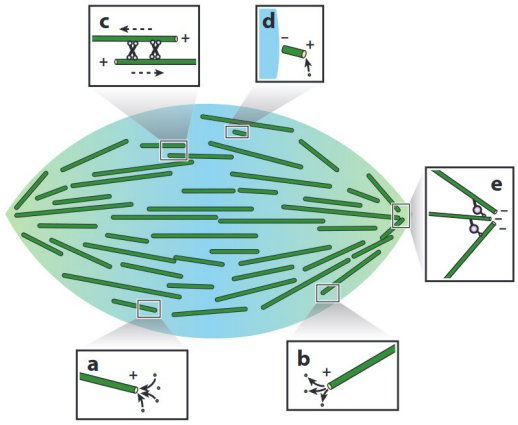

FIG. 3. Sketch of the mitotic spindle showing some of the molecular processes happening at each microtubule: (a) Polymerization (b) De-Polymerization (c) Anti-parallel sliding driven by Kinesin-5 (d) Nucleation near chromosomes (e) Minus end clustering by dynein motors. Borrowed from Fig 2 of ([11])

The key difference from Solon et al ([3]) is that particles will display active transport only in the presence of other anti-parallel particles.

B. Definition of Model

We consider N particles on a 2D lattice of $L_x x L_y$ sites with periodic boundary conditions. Each particle can have spins ± 1 and each site can host any number of particles i.e. there is no excluded volume interaction. The number of particles on each site with spin +1 is denoted by n_i^+ and the number of spins on a site with -1 spin is denoted by n_i^-. We define the total number of particles at a site as $\rho_i = n_i^+ + n_i^-$ and the total magnetisation at a site as $m_i = n_i^+ - n_i^-$. We can therefore write:

$$n_i^+ = \frac{\rho_i + m_i}{2} \qquad n_i^- = \frac{\rho_i - m_i}{2} \tag{1}$$

To describe active nematics using the Active Ising model, we modify the microscopic rules written in Solon et al. [3] to account for the anti-parallel sliding nature of microtubules (See fig 4).We consider a continuous time Markov process where at any given time point, particles choose an action based on the following microscopic rules:

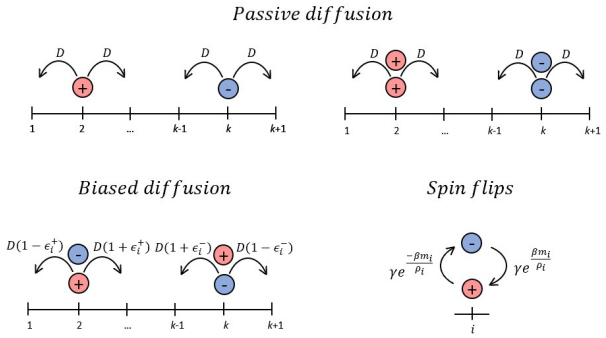

FIG. 4. Sketch of hopping rules with corresponding transition rates. In the absence of spins of opposite signs particles diffuse passively while the presence of opposite spins triggers biased diffusion. "Ferromagnetic" interactions causes spins to flip to align with their fellow spins on same site.

Note that the biased diffusion occurs only along one axis (say x). Particles are free to passively diffuse along the second axis. The primary modification from Solon et al [3] is the introduction of local magnetisation dependence in the biased diffusion. The modifications reflect the anti-parallel sliding of polar rods that can slide only in the presence of anti-parallel rods. We define ϵ_i^+ and ϵ_i^- as:

$$\begin{aligned} \epsilon_i^+ &= \epsilon' \times \frac{n_i^-}{\rho} = \epsilon' \left(\frac{\rho + m}{2\rho} \right) = \epsilon \left(1 + \frac{m}{\rho} \right) \\ \epsilon_i^- &= \epsilon' \times \frac{n_i^+}{\rho} = \epsilon' \left(\frac{\rho - m}{2\rho} \right) = \epsilon \left(1 - \frac{m}{\rho} \right) \end{aligned} \tag{2}$$

The spins therefore, have a mean drift along the x-axis.

$$v_i^+ = 2D\epsilon_i^+ \qquad v_i^- = -2D\epsilon_i^- \tag{3}$$

An interesting consequence of the rules is the local conservation of momentum. i.e.

$$j_i^+ + j_i^- = n_i^+ v_i^+ + n_i^- v_i^- \tag{4}$$

$$j_i^+ + j_i^- = n_i^+ 2D\epsilon_i^+ - n_i^- 2D\epsilon_i^- \tag{5}$$

$$j_i^+ + j_i^- = n_i^+ 2D\epsilon' \left(\frac{n_i^-}{\rho}\right) - n_i^- 2D\epsilon' \left(\frac{n_i^+}{\rho}\right) \tag{6}$$

$$j_i^+ + j_i^- = 0 \tag{7}$$

Such conservation is not seen in conventional polar flocking models where momentum conservation is not built in and the whole system can spontaneously flock in one direction.

C. Order parameter

To describe the state of our system we define the mean magnetization per unit area as our order parameter,

$$m_L = \frac{1}{\rho_0 L_x L_y} \sum_i m_i \tag{8}$$

D. Simulation results

The result of simulations run on Julia are shown in figure (5). The key features of the phase diagram are:

- At high temperatures and low densities we see a homogeneous disordered steady state.
- At low temperatures and high densities we see a homogeneous ordered steady state.
- At intermediate values of temperature and densities we see a homogeneous semi-ordered steady state. At the resolution tested, we see a continuous transition from disorder to order.
- At no point in the parameter space do we see in-homogeneity in the density distribution. This is in contrast to the discontinuous liquid-gas phase transition seen in Solon et al ([3])
- At intermediate parameters we see the occurrence of exotic long-lived meta-stable bands when the system is initialized from a homogeneous disordered state, figure (6).We explore these bands in detail:

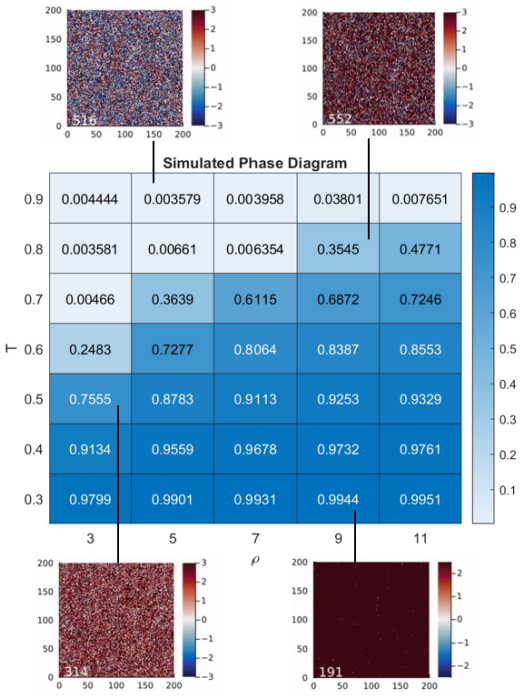

FIG. 5. The value of average magnetization of the system of $\rho.L_x.L_y$ particles in a L_x x L_y box simulated for 1500 time points (γ^{-1} units) starting from the homogeneous ordered phase ($D = r = 1, v = 2, L_x = L_Y = 200$). Steady-state configuration for representative points is shown with the colorbar representing magnetization per site.

1. *Meta-stable Band Formation*

Since our dynamics involved anti-parallel particles sliding along the x-direction, we expected the formation of vertical bands of alternating magnetization. However, to our surprise, we quite often found the formation of horizontal bands of alternating magnetization. Note that this is not a robust phenomenon and different runs at the same parameters might not show band formation. However, close to the transition from the disordered to ordered steady state, band formation is almost always ob-

served when the system is initiated in a homogeneous disordered state.

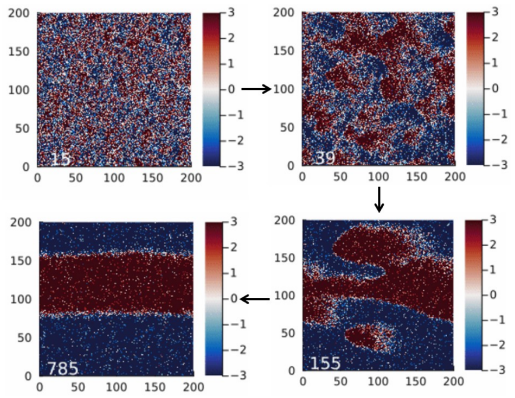

FIG. 6. Meta-stable bands with alternative magnetization are formed when the system is initialized from a homogeneous disordered state ($T = 0.5, \rho = 7$)

E. Meta-stable bands are long lived

The time scale of band formation is roughly 500 steps and our initial hunch was that these bands would quickly dissolve giving rise to uniform magnetisation. However, these bands last up to at least 100,000 time steps! (figure 7). Based on the microscopic dynamics one can build intuition why any fluctuations of the interface will die down because of anti-parallel sliding at the interface where particles of opposite polarization meet.

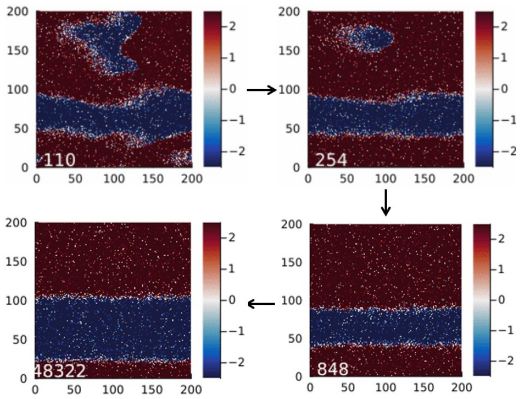

FIG. 7. Meta-stable bands last for upto atlease 100,000 time steps (γ^{-1} units) ($T = 0.5, \rho = 7$)

F. Interfaces of meta-stable bands diffuse over long time scales

Although fluctuations at the interface are damped and the interface remains horizontal, the whole interface is free to diffuse in the y direction. This can be seen in figure (8), where the average magnetization diffuses over extremely long time scales.

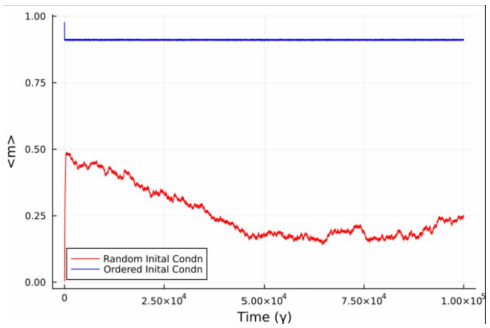

FIG. 8. Over long time scales 100,000 time steps (γ^{-1} units), the inter-membrane space follows diffusive dynamics ($T = 0.5, \rho = 7$)

G. Interfaces are the region of highest momentum

Based on our microscopic rules, particles diffuse actively only in the presence of anti-parallel particles. Therefore, we expect that in the bulk of uniform magnetization, there is lower momentum. At the interface of regions of opposite magnetization we see enhanced momentum as particles of opposite spin diffuse into each other and are actively transported until they flip because of their ferromagnetic interaction with the bulk. A balance of D, v and T sets the thickness of the interface.

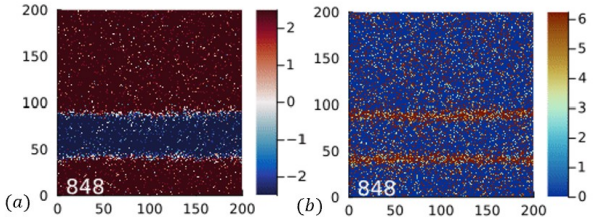

FIG. 9. (a) Steady-state magnetization of horizontal band configuration. (b) Corresponding momentum $J_x^+ = J_x^-$ at the same time point. ($T = 0.5, \rho = 7$)

H. Vertical interfaces are asymmetric

When vertical bands of alternating magnetization appear, the interface where leftward-facing particles meet rightwards facing particles is stable, since any diffusion across the interface is opposed by anti-parallel sliding leading to the formation of sharp interfaces, figure (10). However, when rightwards-facing particles meet leftwards-facing particles any diffusion across the interface is enhanced by anti-parallel sliding leading to the formation of diffused interfaces. I believe this asymmetry is primarily responsible for stabilizing horizontal interfaces since any fluctuation creates two types of vertical interfaces, one of which is unstable and smears out over time.

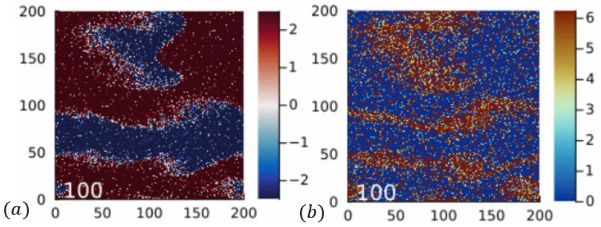

FIG. 10. (a) Transient magnetization state during horizontal band configuration. (b) Corresponding momentum at the same time point. ($T = 0.5, \rho = 7$)

III. HYDRODYNAMIC DESCRIPTION OF THE MODEL

We can derive a continuous description of the modified Active Ising model following [3] and write down coupled partial differential equations for the magnetization and density fields.

A. Mean Field Theory

In 1 D, we can write the evolution of mean number of spins at site i as,

$$\begin{aligned}\left\langle \dot{n}_i^{\pm} \right\rangle &= D\left\langle (1 \pm \varepsilon_i^{\pm}) n_{i-1}^{\pm} \right\rangle + D\left\langle (1 \mp \varepsilon_i^{\pm}) n_{i+1}^{\pm} \right\rangle - 2D\left\langle n_i^{\pm} \right\rangle \\ &\pm \left\langle n_i^{-} \exp\left(\beta \frac{m_i}{\rho_i}\right) \right\rangle \mp \left\langle n_i^{+} \exp\left(-\beta \frac{m_i}{\rho_i}\right) \right\rangle \end{aligned} \tag{9}$$

Using our definition of $\varepsilon_i^{\pm}$ from equation (2) we get,

$$\begin{aligned}\left\langle \dot{n}_i^{\pm} \right\rangle &= D\left\langle (1 \pm \epsilon - \epsilon \frac{m_i}{\rho_i}) n_{i-1}^{\pm} \right\rangle + D\left\langle (1 \mp \pm \epsilon + \epsilon \frac{m_i}{\rho_i}) n_{i+1}^{\pm} \right\rangle \\ &- 2D\left\langle n_i^{\pm} \right\rangle \pm \left\langle n_i^{-} \exp\left(\beta \frac{m_i}{\rho_i}\right) \right\rangle \mp \left\langle n_i^{+} \exp\left(-\beta \frac{m_i}{\rho_i}\right) \right\rangle \end{aligned} \tag{10}$$

Using equation 10 and our definition of ρ_i and m_i we can write,

$$\begin{aligned}\left\langle \dot{\rho}_i \right\rangle &= D\left(\left\langle \rho_{i+1} \right\rangle + \left\langle \rho_{i-1} \right\rangle - 2\left\langle \rho_i \right\rangle\right) - D\varepsilon\left(\left\langle m_{i+1} \right\rangle - \left\langle m_{i-1} \right\rangle\right) \\ &+ D\varepsilon \left\langle \frac{m_i}{\rho_i}\left(\rho_{i+1} - \rho_{i-1}\right) \right\rangle \end{aligned} \tag{11}$$

$$\begin{aligned}\left\langle \dot{m}_i \right\rangle &= D\left(\left\langle m_{i+1} \right\rangle + \left\langle m_{i-1} \right\rangle - 2\left\langle m_i \right\rangle\right) - D\varepsilon\left(\left\langle \rho_{i+1} \right\rangle - \left\langle \rho_{i-1} \right\rangle\right) \\ &+ D\varepsilon \left\langle \frac{m_i}{\rho_i}\left(m_{i+1} - m_{i-1}\right) \right\rangle \\ &+ 2\left\langle \rho_i \sinh\left(\beta \frac{m_i}{\rho_i}\right) \right\rangle - 2\left\langle m_i \cosh\left(\beta \frac{m_i}{\rho_i}\right) \right\rangle \end{aligned} \tag{12}$$

Taking the continuous limit using taylor series to expand the terms we get:

$$\partial_t \left\langle \rho \right\rangle = D\partial_{xx}\left\langle \rho \right\rangle - v\partial_x \left\langle m \right\rangle + v\left\langle \frac{m}{\rho}\partial_x \rho \right\rangle \tag{13}$$

$$\begin{aligned}\partial_t \left\langle m \right\rangle &= D\partial_{xx}\left\langle m \right\rangle - v\partial_x \left\langle \rho \right\rangle + v\left\langle \frac{m}{\rho}\partial_x m \right\rangle \\ &+ \left\langle 2\rho \sinh\frac{\beta m}{\rho} - 2m\cosh\frac{\beta m}{\rho} \right\rangle \end{aligned} \tag{14}$$

where $v = 2D\varepsilon$. Note that our modification to the Active Ising Model leads to the addition of a new magnetization dependent drift term. Taking the mean field limit by neglecting correlations between m and ρ while evaluating the averages and expanding the hyperbolic functions to order of m^2/ρ^2 we get,

$$\partial_t \rho = D\partial_{xx}\rho - v\partial_x m + v\frac{m}{\rho}\partial_x m \tag{15}$$

$$\begin{aligned}\partial_t m &= D\partial_{xx} m - v\partial_x \rho + v\frac{m}{\rho}\partial_x m \\ &+ 2m(\beta - 1) - \alpha\frac{m^3}{\rho^2} \end{aligned} \tag{16}$$

where $\alpha = \beta^2(1-\beta/3)$ ([3]). Going from 1D to 2D results in the minor change from $\partial_x x$ to Δ since the second axis supports purely diffusive dynamics. This give us,

$$\partial_t \rho = D\Delta\rho - v\partial_x m + v\frac{m}{\rho}\partial_x m \tag{17}$$

$$\begin{aligned}\partial_t m = D\Delta m - v\partial_x \rho + v\frac{m}{\rho}\partial_x m \\ + 2m(\beta-1) - \alpha\frac{m^3}{\rho^2}\end{aligned} \tag{18}$$

These are our mean field equations for the modified Active Ising Model. The steady state solutions are:

$$\rho(x) = \rho_0, \quad m(x) = 0 \tag{19}$$

which is linearly stable for $\beta < 1$. For $\beta > 1$, the linearly stable solutions are:

$$\rho = \rho_0, \quad m = \pm\rho_0\sqrt{\frac{2(\beta-1)}{\alpha}} \tag{20}$$

The mean field solution predicts a smooth disorder-to-order transition where the system density and magnetisation stay homogeneous across the transition. However, since our simulation show exotic states as seen in the previous section, we follow [3] to include fluctuations to our mean field equations and refine our theory.

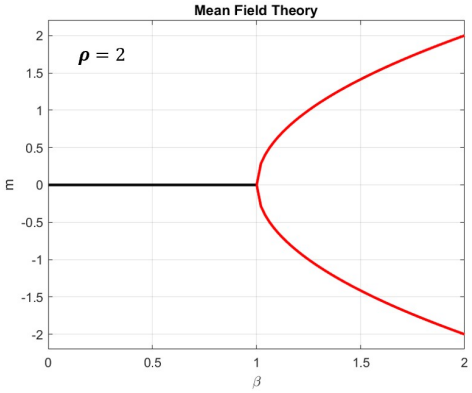

FIG. 11. Linearly stable solution for mean field theory derived in eqn (17),18)

B. Refined Mean Field Theory

In previous section we had replaced all averages with their mean even in the non-linear terms. This overlooks the affect of fluctuations on non-linear terms. Now, we re-derive our mean field theory starting from eqn (13),14) by considering,

$$\mathcal{P}\left[\rho, m; x, t \mid \rho_0, m_0\right] = \mathcal{N}\left(\rho - \bar{\rho}, \alpha_\rho\bar{\rho}\right)\mathcal{N}\left(m - \bar{m}, \alpha_m\bar{\rho}\right) \tag{21}$$

where $\mathcal{N}\left(x, \sigma^2\right) = e^{-x^2/\sigma^2}/\sqrt{2\pi\sigma^2}$ is the normal distribution with σ as the standard deviation. The correction to non-linear terms following [3] are,

$$\left\langle 2\rho\sinh\frac{\beta m}{\rho} - 2m\cosh\frac{\beta m}{\rho}\right\rangle \approx 2\left(\beta - 1 - \frac{r}{\bar{\rho}}\right)\bar{m} - \alpha\frac{\bar{m}^3}{\bar{\rho}^2} \tag{22}$$

where $r = 3\alpha\alpha_m/2$. Following the same procedure on the new drift term ($\left\langle\frac{m}{\rho}\partial_x m\right\rangle$) in our modified Active Ising Model produces a term of the order $1/\rho^2$ which we ignore as all the new phenomenology is captured by the $1/\rho$ term introduced in equation (22). The refined mean field equations are,

$$\partial_t \rho = D\Delta\rho - v\partial_x m + v\frac{m}{\rho}\partial_x m \tag{23}$$

$$\begin{aligned}\partial_t m = D\Delta m - v\partial_x \rho + v\frac{m}{\rho}\partial_x m \\ + 2m\mu - \alpha\frac{m^3}{\rho^2}\end{aligned} \tag{24}$$

where $\mu = \beta - 1 - \frac{r}{\rho}$.

C. Linear stability analysis of Refined Mean Field Theory

The steady solution for the system of equations (23,24) are,

$$\rho(x) = \rho_0, \quad m(x) = 0, \pm\rho_0\sqrt{\frac{2\mu}{\alpha}} \tag{25}$$

We now perform linear stability analysis on the homogeneous disordered phase ($(\rho, m) = (|rho_0, 0)$). We substitute $m(\mathbf{r}, t) = \delta m(\mathbf{r}, t)$, $\rho(\mathbf{r}, t) = \rho_0 + \delta m(\mathbf{r}, t)$ and go into fourier space,

$$\delta\rho = \int_{-\infty}^{\infty} dx \int_{-\infty}^{\infty} dy \delta\rho(\mathbf{q},t) e^{-i(q_x x + q_y y)} \tag{26}$$

Linearizing the resultant equations we get,

$$\partial_t \begin{pmatrix} \delta\rho \\ \delta m \end{pmatrix} = \begin{pmatrix} -D|q|^2 & iq_x v \\ iq_x v & -D|q|^2 + 2\mu_0 \end{pmatrix} \begin{pmatrix} \delta\rho \\ \delta m \end{pmatrix} \tag{27}$$

where $\mu = \beta - 1 - \frac{r}{\rho_0}$. The corresponding eigen values of the matrix in equation (27), calculated using Mathematica are,

$$\lambda_\pm = -D\left(q_x^2 + q_y^2\right) + \mu_0 \pm \sqrt{\mu_0^2 - v^2 q_x^2} \tag{28}$$

The stability of the system is determined by the real part of the eigenvalues which depend on the sign of μ_0. This gives equation for the upper spinodal,

$$\beta - 1 - \frac{r}{\rho} = \frac{1}{T} - 1 - \frac{r}{\rho} = 0 \tag{29}$$

Points that lie below this line in the $T - \rho$ parameter space will be unstable in the homogeneous disordered state. Following the same procedure for the homogeneous ordered phase ($(\rho, m) = (\rho_0, m_0)$). We substitute $m(\mathbf{r},t) = m_0 + \delta m(\mathbf{r},t)$, $\rho(\mathbf{r},t) = \rho_0 + \delta m(\mathbf{r},t)$ and go into fourier space. Linearizing the resultant equations we get,

$$\partial_t \begin{pmatrix} \delta\rho \\ \delta m \end{pmatrix} = A \begin{pmatrix} \delta\rho \\ \delta m \end{pmatrix} \tag{30}$$

where

$$A = \begin{pmatrix} -D|q|^2 - iq_x v\frac{m}{\rho} & iq_x v \\ iq_x v + \frac{m_0}{\rho_0}\left(\frac{2r}{\rho_0} - 4\mu_0\right) & -D|q|^2 - 4\mu_0 - iq_x v\frac{m}{\rho} \end{pmatrix} \tag{31}$$

The eigenvalues of A, from Mathematica are,

$$\lambda_\pm = -D\left(q_x^2 + q_y^2\right) - 2\mu_0 - iq_x v\frac{m}{\rho} \pm \sqrt{4\mu_0^2 - v^2 q_x^2 - \frac{2im_0 q_x v\left(r + 2\mu_0\rho_0\right)}{\rho_0^2}} \tag{32}$$

We note that q_y only has a stabilizing effect. This makes sense since it only supports diffusive dynamics. We set it to 0 for the next steps. Deriving an analytical equation for the spinodal similar to equation (29) is non-trivial. However, by studying $\Re(\lambda_\pm)$ vs q_x as a function of T for each ρ, we can numerically determine the phase space over which the ordered homogeneous state is stable. An example of such a plot is shown in figure (12)

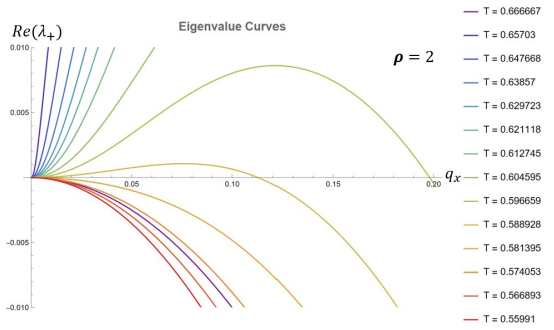

FIG. 12. Real part of largest eigenvalue λ_+ (32) as a function of q_x for $D = r = 1, v = 2, \rho = 2$

For any value of ρ, by systematically decreasing temperature from the upper spinodal line, as calculated in equation (29), we see that there exists a region of temperature where the ordered homogeneous state is unstable. This is an indication of a region where we would expect phase separation! By following the above-mentioned procedure at varying values of ρ, we can build the lower spinodal line as shown in figure (13),

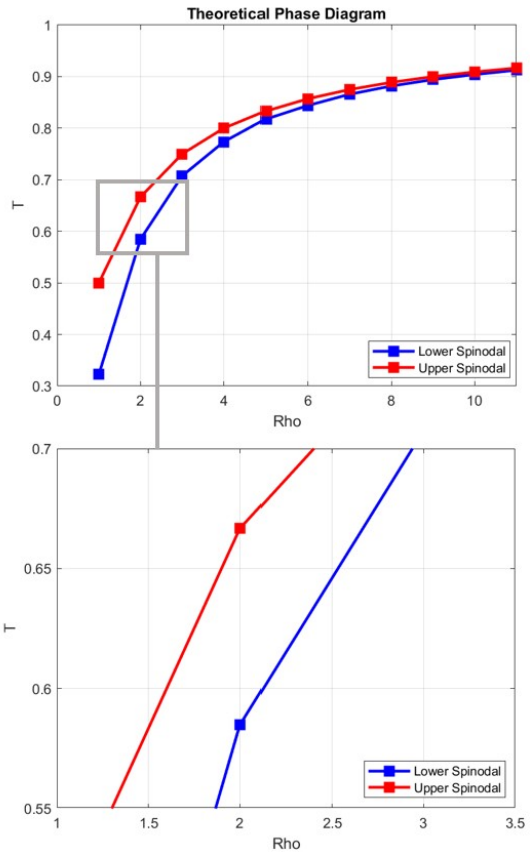

FIG. 13. Phase diagram of the refined mean field theory of the modified Active Ising Model indicating the spinodal denoting the limits of linear stability of the homogeneous profiles ($D = r = 1, v = 2$)

Since the above analysis predicts the existence of a parameter regime where the homogeneous state is unstable, we do a more thorough sweep of our phase diagram to search for such a region, figure (14)

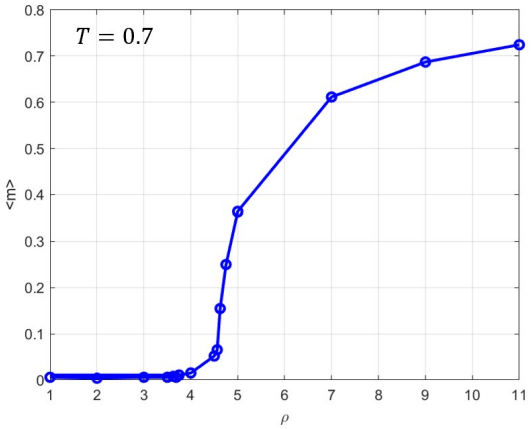

FIG. 14. Steady state magnetization after 1500 time steps (γ^{-1}) units for $T = 0.7$ as a function of ρ ($D = r = 1, v = 2$)

Our results show a continuous square root-like dependence of magnetization on the particle density with no sign of phase separation at the parameters explored.

IV. DISCUSSION

Reproducing the phenomenology of active nematics with a lattice model is non-trivial. The above model, motivated by biological insight, attempts to modify the microscopic rules of the Active Ising Model to reproduce the collective behaviour seen in microtubule-motor protein mixtures. Constrained by local conservation of momentum, our model does not show global uni-directional translation as seen in the original Active Ising Model. We report the existence of long-lived, metastable bands of opposite polarisation with asymmetric interfaces. Our refined mean-field theory predicts the existence of a region of phase separation which we were unable to find in our simulations. This could be either due to a mistake in the theoretical estimation of the phase diagram or an incomplete survey of our parameters space. This project reveals how insights from biological experiments can inspire the development of new physical theories with unpredictable results. It would be interesting to extend the above model from a q=2 system to q=4. It would also be exciting to solve the coupled nemato-hydrodynamics equations on a lattice to more truthfully capture the phenomenology of Active Nematics.

V. ACKNOWLEDGMENTS

I thank Dr Sunghan Ro for sharing his Julia code for the original Active Ising Model. I am also grateful to him for useful discussion and guidance throughout the project. I thank Prof Mehran Kardar and Changnan Peng for a great course. I also thank Prof Mehran Kardar for an amazing 3-course series on Statistical Mechanics which will prove to be a cornerstone in my graduate training.

[1] A. Doostmohammadi, J. Ignés-Mullol, J. M. Yeomans, and F. Sagués, Active nematics, Nature communications **9**, 3246 (2018).

[2] A. P. Solon and J. Tailleur, Revisiting the flocking transition using active spins, Physical review letters **111**, 078101 (2013).

[3] A. P. Solon and J. Tailleur, Flocking with discrete symmetry: The two-dimensional active ising model, Physical Review E **92**, 042119 (2015).

[4] C. W. Reynolds, Flocks, herds and schools: A distributed behavioral model, in *Proceedings of the 14th annual conference on Computer graphics and interactive techniques* (1987) pp. 25–34.

[5] T. Vicsek, A. Czirók, E. Ben-Jacob, I. Cohen, and O. Shochet, Novel type of phase transition in a system of self-driven particles, Physical review letters **75**, 1226 (1995).

[6] J. Toner and Y. Tu, Flocks, herds, and schools: A quantitative theory of flocking, Physical review E **58**, 4828 (1998).

[7] J. Toner, Y. Tu, and S. Ramaswamy, Hydrodynamics and phases of flocks, Annals of Physics **318**, 170 (2005).

[8] Z. Csahók and T. Vicsek, Lattice-gas model for collective biological motion, Physical Review E **52**, 5297 (1995).

[9] T. Sanchez, D. T. Chen, S. J. DeCamp, M. Heymann, and Z. Dogic, Spontaneous motion in hierarchically assembled active matter, Nature **491**, 431 (2012).

[10] R. Aditi Simha and S. Ramaswamy, Hydrodynamic fluctuations and instabilities in ordered suspensions of self-propelled particles, Phys. Rev. Lett. **89**, 058101 (2002).

[11] B. J. Oriola D, Needleman DJ, The physics of the metaphase spindle, Annu Rev Biophys. **20**, 655 (2018).